Rosenbluth Separation in the Continuum Region

Alain Romeyer [a]

[a] *Institut des Sciences Nucléaires*
IN2P3-CNRS/Université Joseph Fourier
38026 Grenoble cedex, France

Abstract

An empirical method for the optimization of the acceptance in missing energy for E89-044 kinematics is presented. It is found that systematic shifts of the central ray of the electron and hadron spectrometers allow to reach higher missing energy, and to access a Rosenbluth separation in the continuum region, in most cases.

1 Introduction

The understanding of the reaction mechanisms involved in the ^{3}He(e,e′p)pn process calls for a Rosenbluth separation in the widest missing energy and momentum domain. Indeed, even if the dominant process involving the interaction of the virtual photon with a correlated nucleon pair has been experimentally observed [1], a recent Rosenbluth separation [2] has shown that the experimental ratio of the longitudinal and transverse response function is not consistent with a complete calculation taking care of Final State Interaction and Meson Exchange Currents. Some important mechanisms and/or corrections are missing, knowledge of which would definitely benefit from a Rosenbluth separation at higher missing energy and momentum.

Up to now, the kinematics settings of the E89-044 experiment has been guided by the optimization of the Rosenbluth separation for pd breakup of ^{3}He in the quasielastic peak region. The purpose of this report is to show that some minor modifications in the electron and hadron spectrometers settings allow for a larger coverage of the continuum region, while keeping the same quality of the Rosenbluth separation in the small missing energy region.
The optimization procedure is developped in the next section. The results of Monte Carlo simulations performed with MCEEP [3] are presented and discussed in Sect. 3. Sect. 4 gives the conclusions.

2 Optimization Procedure

The missing energy parameter E_m for the reaction A(e,e′p)B is an experimental quantity representing the separation energy of the proton. This parameter may be written, in terms of the known and/or measured quantities

$$E_m = E - E' - T_p - T_B \tag{1}$$

where $(\vec{k}, E)$ and $(\vec{k}', E')$ are the incident and scattered electron 4-momentum, $(\vec{p}, E_p = T_p + m_p)$ is the proton 4-momentum and T_B is the kinetic energy of the recoiling system. This last quantity can be expressed in terms of the known and/or measured quantities according to

$$T_B = \omega + m_A - E_p - \sqrt{(\omega + m_A - E_p)^2 - p_m^2} \tag{2}$$

where $(\vec{q} = \vec{k} - \vec{k}', \omega = E - E')$ is the 4-momentum of the virtual photon and $\vec{p}_m = \vec{q} - \vec{p}$ is the missing momentum, that is the 3-momentum of the recoiling system.
The continuum region corresponds to the kinematical region relevant to the ^{3}He(e,e′p)pn process, characteristic missing energy of which satisfies

$$7.718 \text{ MeV} \leq E_m^{\text{cont.}} \leq 140 \text{ MeV} \tag{3}$$

while the 2-body breakup peak corresponds to the constant missing energy

$$E_m^{pd} = 5.494 \text{ MeV} . \tag{4}$$

Fig. 1 shows a typical missing energy distribution of the allowed phase space for a selected kinematics of the ^{3}He(e,e′p)pn reaction. This distribution exhibits a characteristic trapezoidal shape, almost symetrical with respect to $E_m = 0$. The width of the trapeze reflects the acceptances of the spectrometers and amounts about $2\,(\Delta E' + \Delta T_p)$. The plateau ranges from $E_m|_{min}$ up to $E_m|_{max}$ corresponding to the missing energies

$$E_m|_{min} \equiv E_m(E' - \Delta E', T_p + \Delta T_p) \tag{5}$$
$$E_m|_{max} \equiv E_m(E' + \Delta E', T_p - \Delta T_p) \tag{6}$$

obtained by substituting E' and T_p by their indicated values in Eq. (1). A large part of the spectrum consists of negative missing energy values, allowed by a phase space calculation but experimentally non-observed since a typical E_m spectrum for the E89-044 experiment should start at E_m^{pd}. Only accidental e-p coincidences can generate *events* in the negative E_m region. Therefore, a shift of the E_m spectrum up to $E_m|_{min} = 0$ would not only allows a more efficient use of the spectrometers but would also lead to an increase of $E_m|_{max}$, improving thus the coverage of the continuum region.

According to Eq. 1, the missing energy spectrum could be shifted towards higher values by three different means:

i) an increase of the beam energy;
ii) a decrease of the scattered electron energy;
iii) a decrease of the proton kinetic energy.

Since the tuning of the beam energy cannot be considered as a viable solution, an independent shift of E' and T_p succeed. The optimization of these shifts is nevertheless constrained by some physics criteria specific of the Rosenbluth separation method:

i) the proton kinetic energy at forward and backward angles have to be the same;
ii) the separation will be done only if the (E_m, p_m) phase space for the Rosenbluth separation have maximum overlap.

These requirements clearly support the following method:

i) the proton kinetic energy shift is optimized at backward kinematics, that is in a region where the scattered electron energy is too small to modify efficiently E_m;
ii) keeping this new setting of the hadron spectrometer, the scattered electron energy is then optimized at forward angles;
iii) the optimum phase space for the Rosenbluth separation is then determined with respect to $E_m|_{max}$ together with eventual additional constraints deduced from the matching of the forward and backward phase spaces.

3 Monte-Carlo Simulations

3.1 Missing Energy and Rosenbluth Phase Space

The optimization method developed previously is based on extensive simulations of the ^{3}He(e,e'p)pn reaction using MCEEP [3]. Each single kinematics of the E89-044 experiment was simulated and optimized with respect to the available (E_m, p_m) phase space for the Rosenbluth separation.

Tables 1 and 2 give the start values of $E_m|_{max}$ and of the Rosenbluth phase space (RPS) determined from Fig. 2-12. Here, the central ray of the electron and hadron spectrometers correspond to the perpendicular and parallel kinematics settings of Ref. [4]. Tables 3 and 4 indicate the same parameters for the quoted optimized shifts of the spectrometers, as determined from

Fig. 2-12 according to the presented optimization procedure. The different curve on these figures serve the location of the 2-body breakup and of the continuum correlations in the (E_m, p_m) phase space; in addition, the comparison between forward and backward angles allow to check the consistency of the determined RPS.

Table 1: central perpendicular kinematics.

Kinematics					Phase Space	LT Separation		
Kin.		p_m (MeV/c)	E′ (GeV)	p (GeV/c)	$E_m\|_{max}$ (MeV)	$E_m\|_{max}$ (MeV)	$p_m\|_{min}$ (MeV/c)	$p_m\|_{max}$ (MeV/c)
1	Σ_1	0	3.9585	1.500	125	50	0	115
2	Σ_2	0	3.9585	1.500	125	50	0	115
3	Σ_3	0	0.4085	1.500	50	50	0	115
4	Σ_1	150	3.9585	1.493	120	50	100	225
5	Σ_2	150	3.9585	1.493	130	50	100	225
6	Σ_3	150	0.4085	1.493	50	50	100	225
7	Σ_1	300	3.9585	1.472	100	45	250	370
8	Σ_2	300	3.9585	1.472	170	45	250	370
9	Σ_3	300	0.4085	1.472	45	45	250	370
10	Σ_1	425	3.9585	1.444	100	45	370	470
11	Σ_2	425	3.9585	1.444	170	45	370	470
12	Σ_3	425	0.4085	1.444	45	45	370	470
13	Σ_1	550	3.9585	1.406	100	45	490	530
14	Σ_2	550	3.9585	1.406	180	45	490	530
15	Σ_3	550	0.4085	1.406	45	45	490	530

Table 2: central parallel kinematics.

Kinematics					Phase Space	LT Separation		
Kin.		p_m (MeV/c)	E′ (GeV)	p (GeV/c)	$E_m\|_{max}$ (MeV)	$E_m\|_{max}$ (MeV)	$p_m\|_{min}$ (MeV/c)	$p_m\|_{max}$ (MeV/c)
16	Σ_1	0	3.607	1.000	130	15	0	100
17	Σ_3	0	0.557	1.000	15	15	0	100
18	Σ_1	0	3.495	2.026	80	50	0	175
19	Σ_3	0	0.745	2.026	50	50	0	175
20	Σ_1	0	2.585	2.999	20	20	0	230
21	Σ_3	0	0.685	2.999	100	20	0	230
22	Σ_1	-300	2.195	1.307	60	50	Refer to Fig. 10	
23	Σ_3	-300	0.295	1.307	50	50	Refer to Fig. 10	
24	Σ_1	-300	3.195	2.327	45	45	Refer to Fig. 11	
25	Σ_3	-300	0.445	2.327	90	45	Refer to Fig. 11	
26	Σ_1	300	3.645	0.913	120	10	280	345
27	Σ_3	300	0.595	0.913	10	10	280	345

In the case of perpendicular kinematics, the shift of the central ray of the spectrometers is substantially increasing $E_m|_{max}$ and RPS. However, RPS stays limited to a part of the continuum region because of the small E_m acceptance at backward angles. Furthermore, the coverage of the continuum region depends on p_m in such a way that, at high missing momenta the (E', T_p) shift does not allow RPS to reach the continuum correlation curve. A dedicated measurement

at backward angles and high missing momenta is mandatory.
The parallel kinematics case is somewhat similar to the perpendicular one. Except the singular case of Kin. 16-17 which exhibits a very narrow plateau at backward angles, the coverage of the continuum region and RPS are always improved. At high positive p_m, the (E', T_p) shift fails to improve the phase space. Once again, a devoted measurement at backward angles would be here necessary.

Table 3: shifted perpendicular kinematics.

Kinematics					Phase Space	LT Separation		
Kin.		p_m (MeV/c)	E' (GeV)	p (GeV/c)	$E_m\|_{max}$ (MeV)	$E_m\|_{max}$ (MeV)	$p_m\|_{min}$ (MeV/c)	$p_m\|_{max}$ (MeV/c)
1	Σ_1	0	3.8885	1.4645	225	70	0	130
2	Σ_2	0	3.8885	1.4645	200	70	0	130
3	Σ_3	0	0.4085	1.4645	70	70	0	130
4	Σ_1	150	3.8935	1.4575	200	70	110	230
5	Σ_2	150	3.8935	1.4575	220	70	110	230
6	Σ_3	150	0.4085	1.4575	70	70	110	230
7	Σ_1	300	3.8715	1.4363	200	70	240	380
8	Σ_2	300	3.8715	1.4363	250	70	240	380
9	Σ_3	300	0.4085	1.4363	70	70	240	380
10	Σ_1	425	3.8915	1.4081	110	70	370	480
11	Σ_2	425	3.8915	1.4081	250	70	370	480
12	Σ_3	425	0.4085	1.4081	70	70	370	480
13	Σ_1	550	3.8985	1.4819	140	55	480	565
14	Σ_2	550	3.8985	1.4819	250	55	480	565
15	Σ_3	550	0.4085	1.4819	55	55	480	565

Table 4: shifted parallel kinematics.

Kinematics					Phase Space	LT Separation		
Kin.		p_m (MeV/c)	E' (GeV)	p (GeV/c)	$E_m\|_{max}$ (MeV)	$E_m\|_{max}$ (MeV)	$p_m\|_{min}$ (MeV/c)	$p_m\|_{max}$ (MeV/c)
16	Σ_1	0	3.497	0.996	220	30	0	110
17	Σ_3	0	0.557	0.996	30	30	0	110
18	Σ_1	0	3.450	1.982	150	80	0	200
19	Σ_3	0	0.745	1.982	80	80	0	200
20	Σ_1	0	2.660	2.904	50	50	0	250
21	Σ_3	0	0.685	2.904	170	50	0	250
22	Σ_1	-300	2.177	1.270	120	80	Refer to Fig.10	
23	Σ_3	-300	0.295	1.270	80	80	Refer to Fig.10	
24	Σ_1	-300	3.255	2.241	80	80	Refer to Fig.11	
25	Σ_3	-300	0.445	2.241	170	80	Refer to Fig.11	
26	Σ_1	300	3.535	0.899	200	30	275	355
27	Σ_3	300	0.595	0.899	30	30	275	355

3.2 Energy Shifts

The mean shifts of the central ray of the electron and hadron spectrometers are 70 Mev and 30(40) MeV, respectively. These changes suffice to produce the needed shift of the missing energy distribution for perpendicular(parallel) kinematics.

Table 5: electron and proton shifts.

Kinematics		Shift	
Kin.		ΔT_p (MeV)	$\Delta E'$ (Mev)
1	Σ_1	30.0	70.0
2	Σ_2	30.0	70.0
3	Σ_3	30.0	0.0
4	Σ_1	30.7	65.0
5	Σ_2	30.7	65.0
6	Σ_3	30.7	0.0
7	Σ_1	30.2	87.0
8	Σ_2	30.2	87.0
9	Σ_3	30.2	0.0
10	Σ_1	29.5	67.0
11	Σ_2	29.5	67.0
12	Σ_3	29.5	0.0
13	Σ_1	63.6	60.0
14	Σ_2	63.6	60.0
15	Σ_3	63.6	0.0
16	Σ_1	4.0	110.0
17	Σ_3	4.0	0.0
18	Σ_1	39.9	45.0
19	Σ_3	39.9	0.0
20	Σ_1	90.5	75.0
21	Σ_3	90.5	0.0
22	Σ_1	29.9	18.0
23	Σ_3	29.9	0.0
24	Σ_1	79.5	60.0
25	Σ_3	79.5	0.0
26	Σ_1	9.7	110.0
27	Σ_3	9.7	0.0

The precise control of the experiment asks for as less as possible changes in the electron arm during the data taking of perpendicular kinematics. Particularly, it is expected to use the single electron rates as a relative luminosity monitor. Consequently, one single scattered electron energy need to be determined for all forward perpendicular kinematic (3.8885 GeV possibly).

3.3 Integrated Rosenbluth Phase Space

The ratio of the integrated RPS to the full $(\mathrm{E_m}, \mathrm{p_m})$ phase space covered for each kinematics setting, is an additional parameter to test the efficiency of the RPS optimization. Since the shift of the spectrometers intends to move the plateau region within the experimentally accepted $(\mathrm{E_m}, \mathrm{p_m})$ phase space, this ratio must increase. An optimum RPS should therefore correspond to a larger ratio.

The ratios for each individual kinematics setting are given in Table 5 for the central and shifted cases. As expected, they are larger for shifted kinematics than for central one. Figures for Kin. 26-27 confirm the failure of the shifting process while other peculiar kinematics are not pinned down by the ratio parameter. Nevertheless, the global result of the optimization procedure is positive: the number of accepted events increases and consequently the statistical uncertainty is expected to decrease.

Table 6: integrated RPS ratio.

Kinematics Kin.		RPS Ratio Central Kin. (%)	RPS Ratio Shifted Kin. (%)
1	Σ_1	4.01	6.57
2	Σ_2	4.01	6.57
3	Σ_3	43.03	63.6
4	Σ_1	5.99	9.85
5	Σ_2	7.66	9.70
6	Σ_3	42.87	61.86
7	Σ_1	6.81	13.66
8	Σ_2	7.77	12.7
9	Σ_3	37.75	63.83
10	Σ_1	5.56	11.49
11	Σ_2	6.40	10.63
12	Σ_3	33.55	57.14
13	Σ_1	1.87	6.05
14	Σ_2	2.55	5.68
15	Σ_3	10.27	31.40
16	Σ_1	1.34	3.24
17	Σ_3	23.85	43.86
18	Σ_1	9.75	17.77
19	Σ_3	30.87	51.30
20	Σ_1	6.50	15.07
21	Σ_3	8.12	20.76
22	Σ_1	6.93	19.02
23	Σ_3	42.42	73.24
24	Σ_1	7.84	13.81
25	Σ_3	20.23	39.30
26	Σ_1	1.05	3.49
27	Σ_3	11.37	37.79

One could also compare the ratios at forward and backward angles. In perpendicular kinematics, an average factor of 6-7 in favour of backward angles is observed; it is correlated to the difference bewteen the small (backward) and the large (forward) scattered electron energy. The present value indicates a better than expected matching of the spectrometer acceptances. This feature must nevertheless be considered cautiously since additional event rejection (q

and ω windows...) might produce a less favourable matching.
In parallel kinematics, the forward/backward matching factor is much more depending on the choice of the settings: the effect of the different scattered electron energies competes with the very narrow E_m plateau influence, leading accordingly to a small or a large factor. The RPS optimization does not really change this figures.

4 Conclusions

An optimization procedure based on acceptance calculations using MCEEP has been developed to access higher missing energies and improve the available phase space for a Rosenbluth separation. A small change of the central ray of the electron and hadron spectrometers suffice to shift the missing energy distribution towards the continuum region. In addition these shifts allow to improve the RPS statistics. For the few kinematics where this method does not give satisfactory results, a third experimental point dedicated to the continuum study is necessary.

In the perpendicular case, the most appropriate experimental method would be to set the electron arm at a fixed value for all forward (or backward) kinematics. In addition, this optimization is only dealing with the change of the proton kinetic energy and of the scattered electron energy. One could also consider the change of the angle of the hadron spectrometer, particularly for parallel kinematics in order to align with the virtual photon. This obviously suggests a second iteration of the presented optimization results.

References

[1] C. Marchand *et al.*, *Phys. Rev. Lett.* **60** (1988) 1703.

[2] J.M. Le Goff *et al.*, *Phys. Rev.* **C55** (1997) 1600.

[3] P. Ulmer, *Monte Carlo for Electro-Nuclear Coincidence Experiments* **v2.3** (1999).

[4] http://www.jlab.org/~kuss/e89044/e89044.html

Figure Captions

Figure 1: typical central missing energy acceptance distribution (full line), together with its shifted partner (dashed line) according to the proposed optimization procedure.

Figure 2: comparison of the Σ_i phase space for the perpendicular kinematics settings of Kin. 1-3; the first and second row of histograms correspond to the central and the shifted kinematics, respectively; the green curve indicate the location of the 2body breakup events; the blue curve show the correlation between the missing energy and the missing momentum when the reaction occurs on a pair of correlated nucleons; the red lines limit the useful (E_m,p_m) region for the Rosenbluth separation.

Figure 3: same as Fig. 2 for Kin. 4-6.

Figure 4: same as Fig. 2 for Kin. 7-9.

Figure 5: same as Fig. 2 for Kin. 10-12.

Figure 6: same as Fig. 2 for Kin. 13-15.

Figure 7: comparison of the Σ_i phase space for the parallel kinematics settings of Kin. 16-17; the different rows and coloured curves have the same meaning as previously.

Figure 8: same as Fig 7 for Kin. 18-19.

Figure 9: same as Fig 7 for Kin. 20-21.

Figure 10: same as Fig 7 for Kin. 22-23.

Figure 11: same as Fig 7 for Kin. 24-25.

Figure 12: same as Fig 7 for Kin. 26-27.

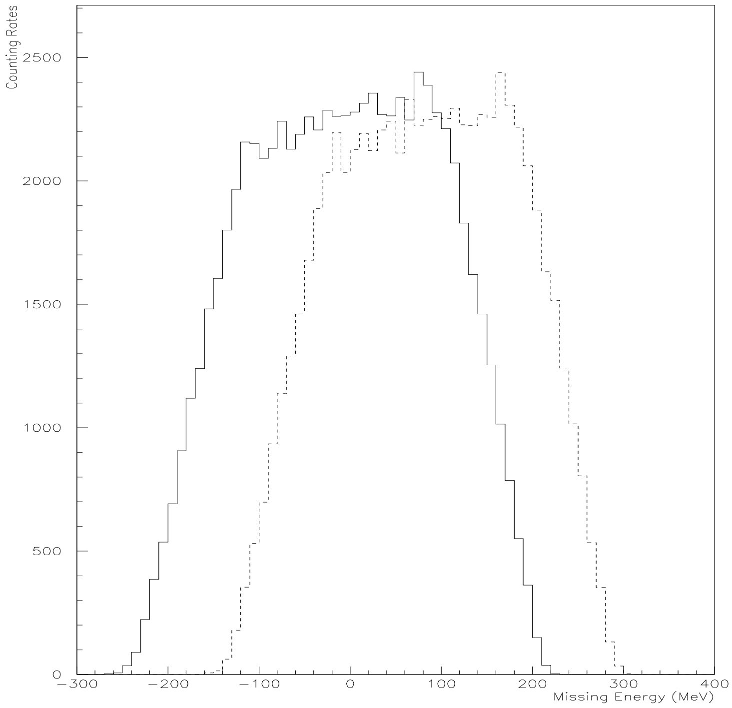
Counting Rates
2500
2000
1500
1000
500
0
−300
−200
−100
0
100
200
300
400
Missing Energy (MeV)

Figure 1.

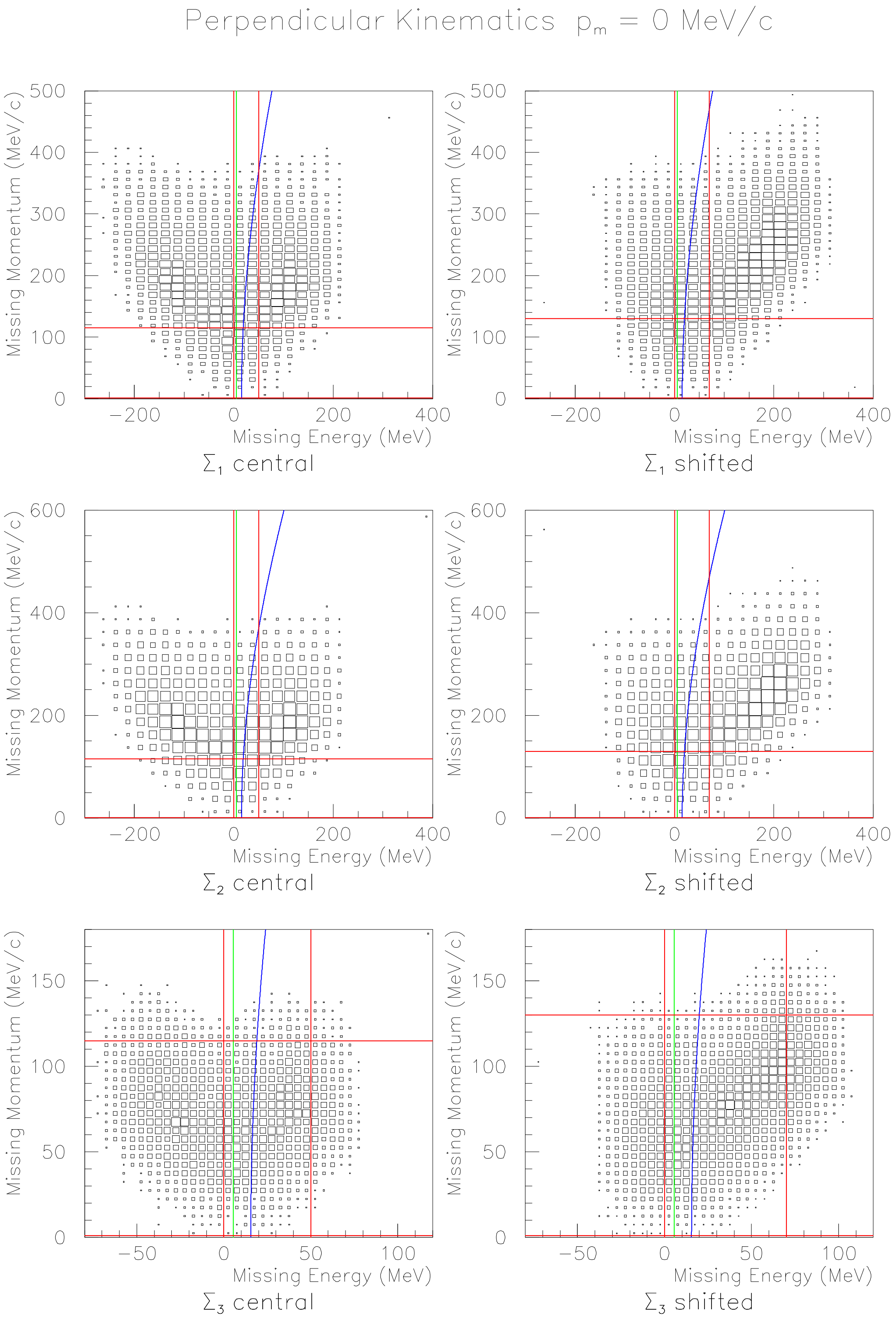
Perpendicular Kinematics p_m = 0 MeV/c
Missing Momentum (MeV/c)
Missing Energy (MeV)
Σ_1 central
Σ_1 shifted
Σ_2 central
Σ_2 shifted
Σ_3 central
Σ_3 shifted

Figure 2.

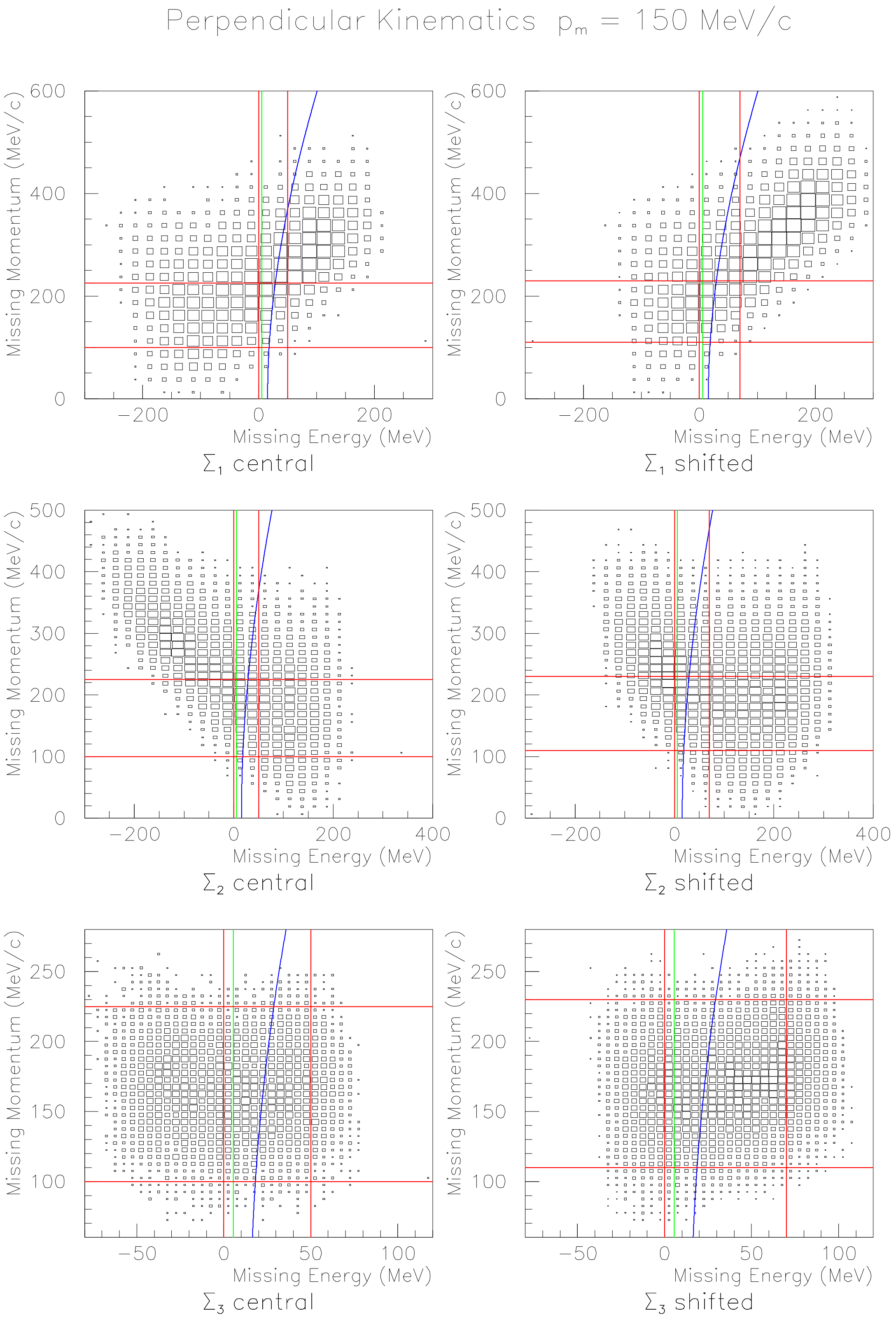
Perpendicular Kinematics p_m = 150 MeV/c
Missing Momentum (MeV/c)
Missing Energy (MeV)
Σ_1 central
Σ_1 shifted
Σ_2 central
Σ_2 shifted
Σ_3 central
Σ_3 shifted

Figure 3.

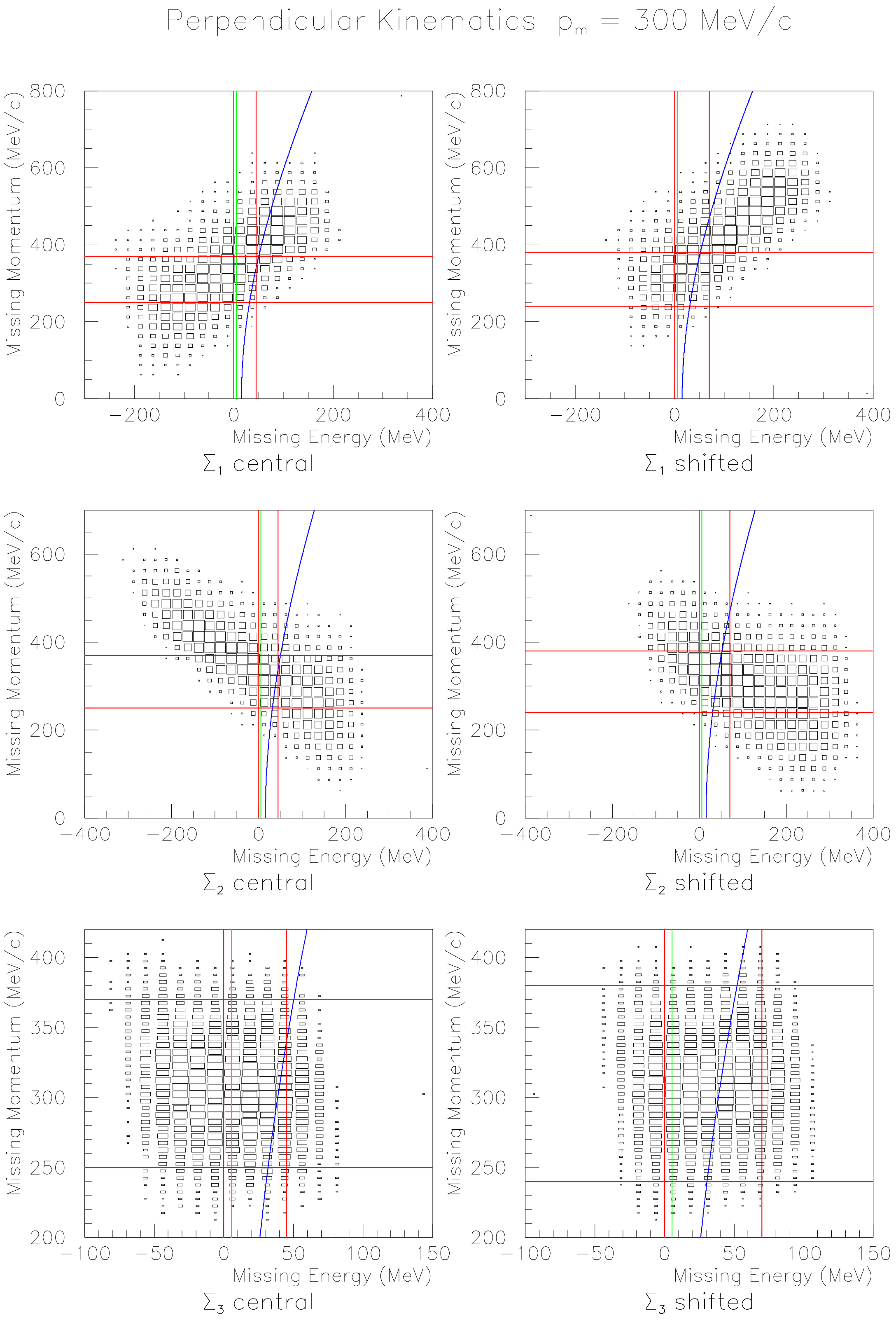

Perpendicular Kinematics p_m = 300 MeV/c
Missing Momentum (MeV/c)
Missing Energy (MeV)
Σ_1 central
Σ_1 shifted
Σ_2 central
Σ_2 shifted
Σ_3 central
Σ_3 shifted

Figure 4.

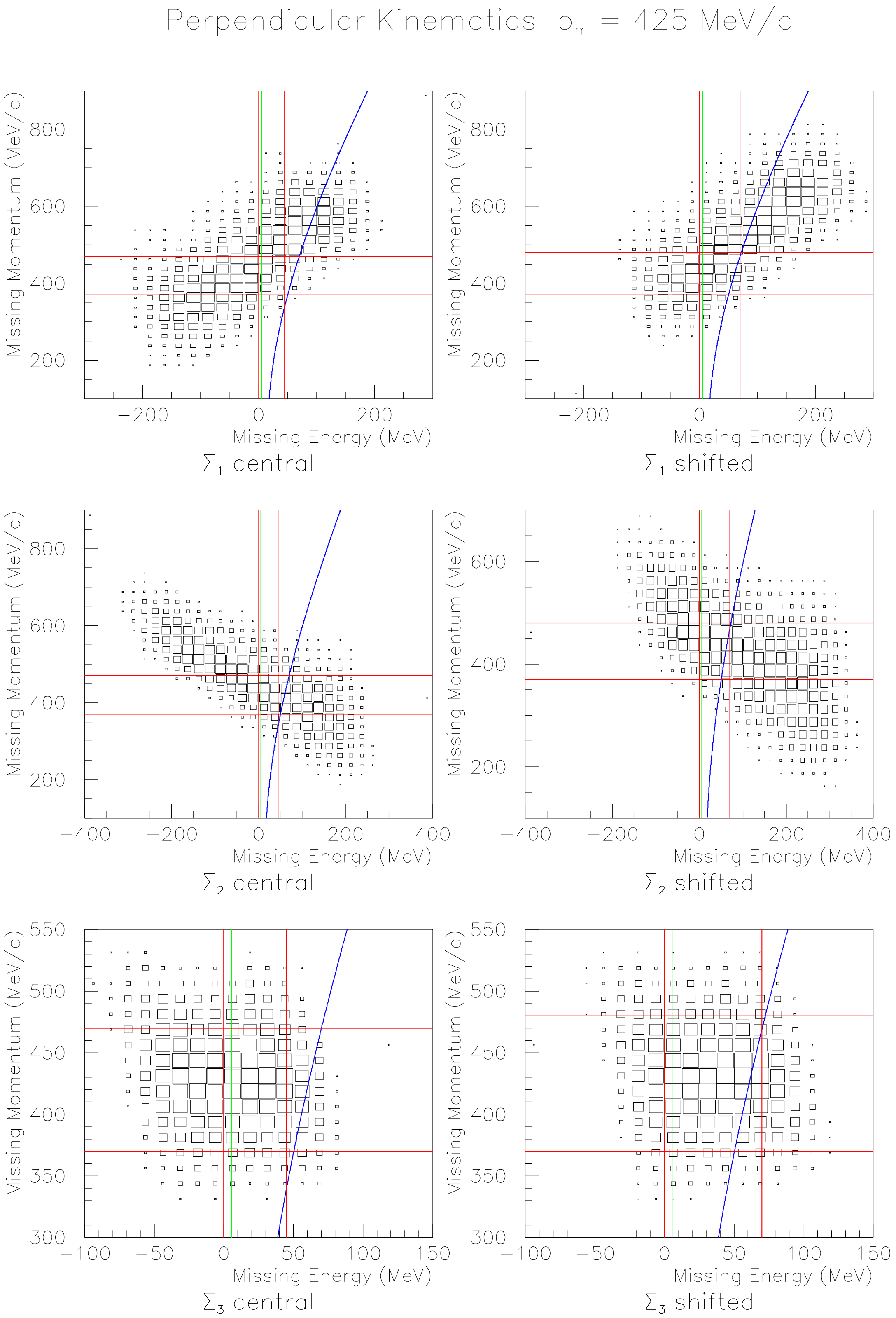
Perpendicular Kinematics p_m = 425 MeV/c
Missing Momentum (MeV/c)
Missing Energy (MeV)
Σ_1 central
Σ_1 shifted
Σ_2 central
Σ_2 shifted
Σ_3 central
Σ_3 shifted

Figure 5.

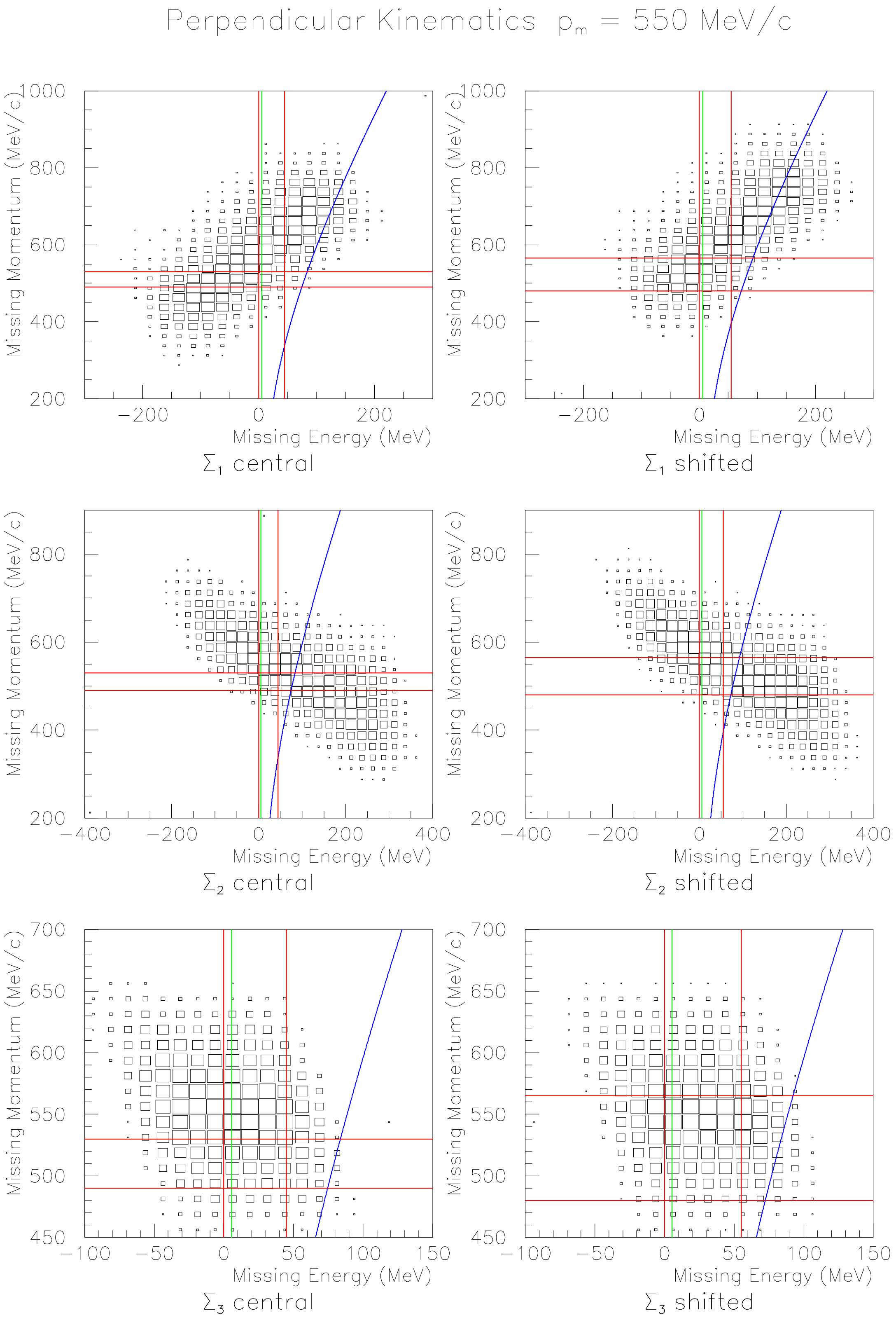

Perpendicular Kinematics p_m = 550 MeV/c
Missing Momentum (MeV/c)
Missing Energy (MeV)
Σ_1 central
Σ_1 shifted
Σ_2 central
Σ_2 shifted
Σ_3 central
Σ_3 shifted

Figure 6.

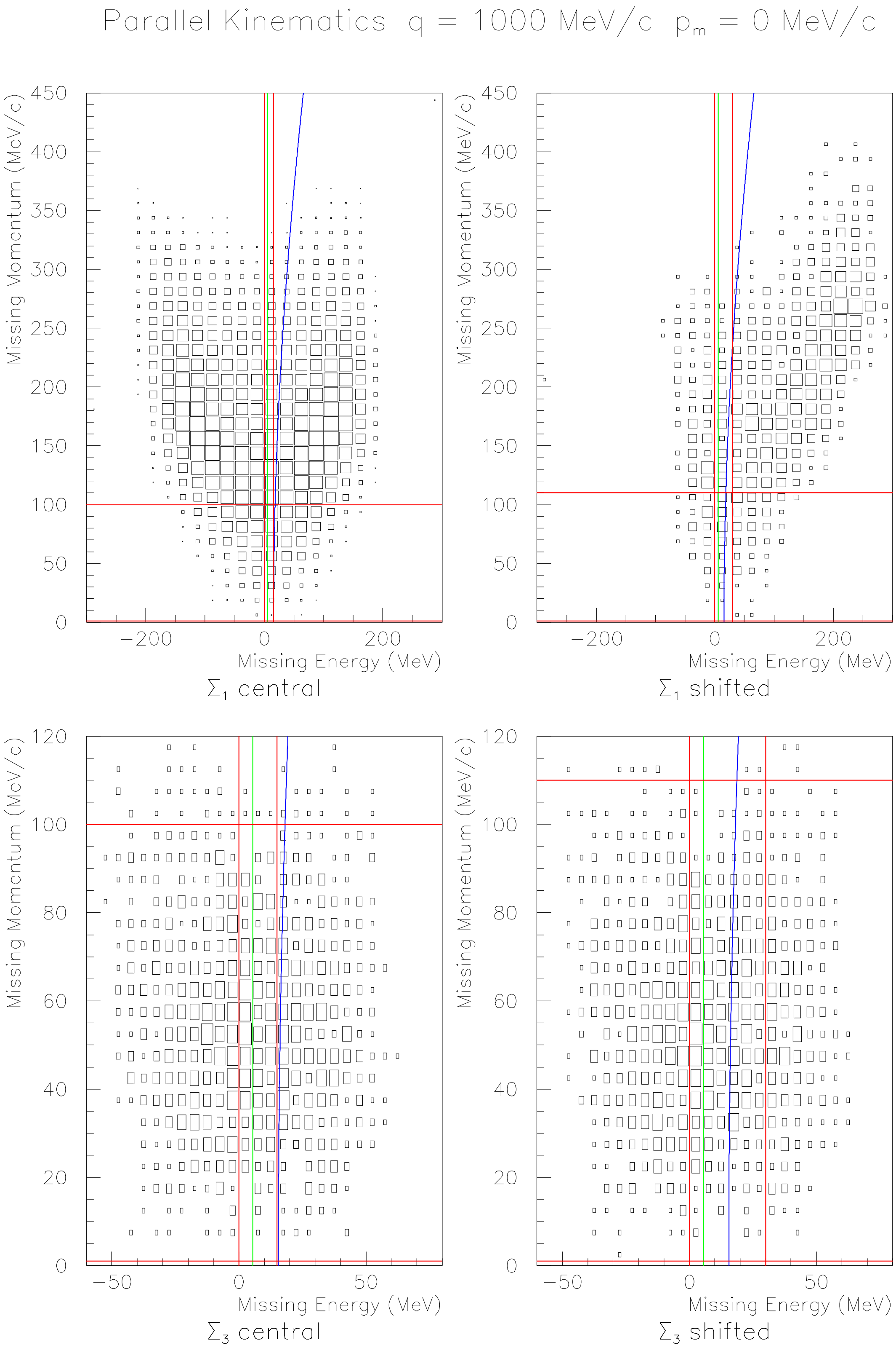
Parallel Kinematics q = 1000 MeV/c p$_m$ = 0 MeV/c
Missing Momentum (MeV/c)
Missing Energy (MeV)
Σ_1 central
Σ_1 shifted
Σ_3 central
Σ_3 shifted

Figure 7.

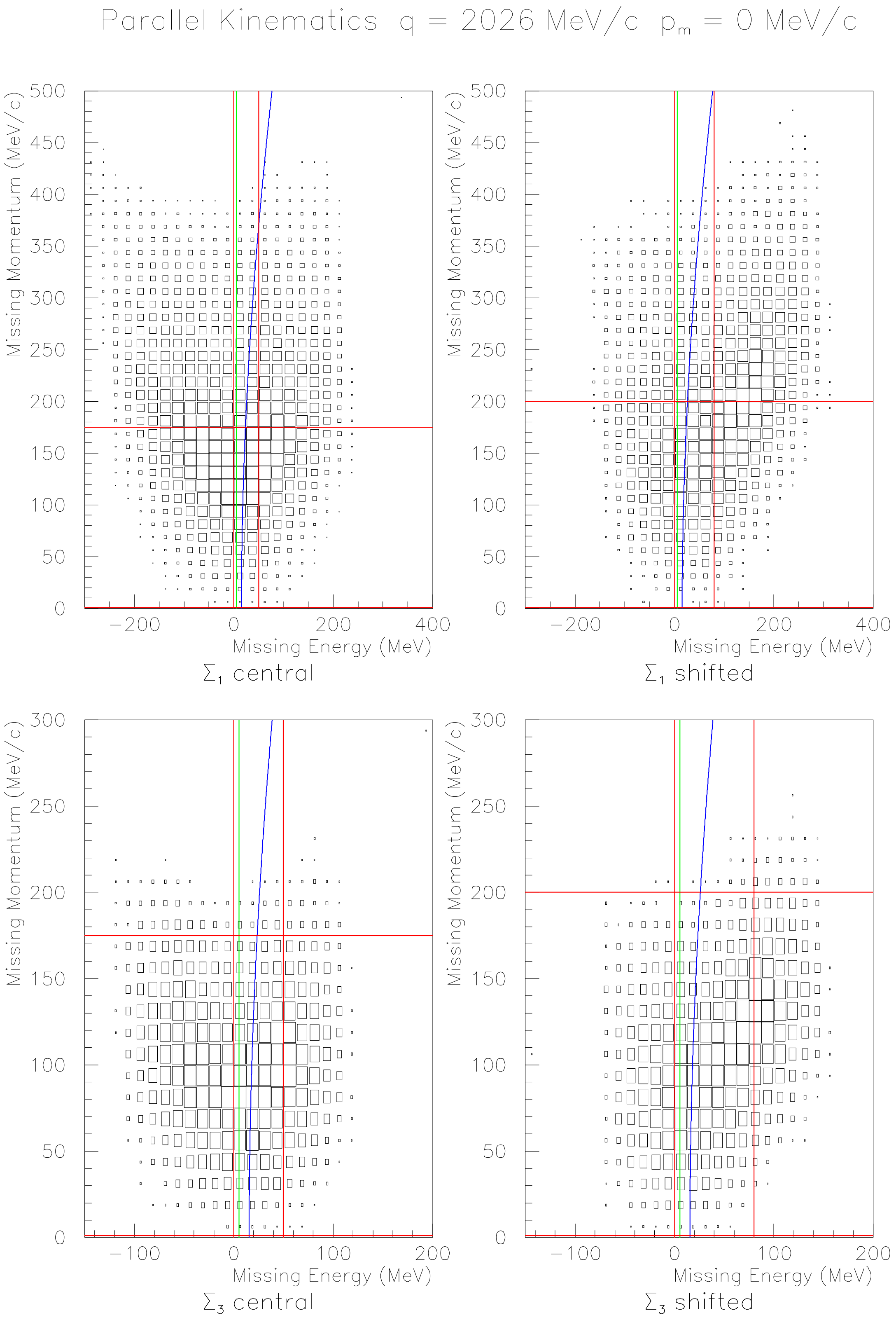

Parallel Kinematics q = 2026 MeV/c p_m = 0 MeV/c
Missing Momentum (MeV/c)
Missing Energy (MeV)
Σ1 central
Σ1 shifted
Σ3 central
Σ3 shifted

Figure 8.

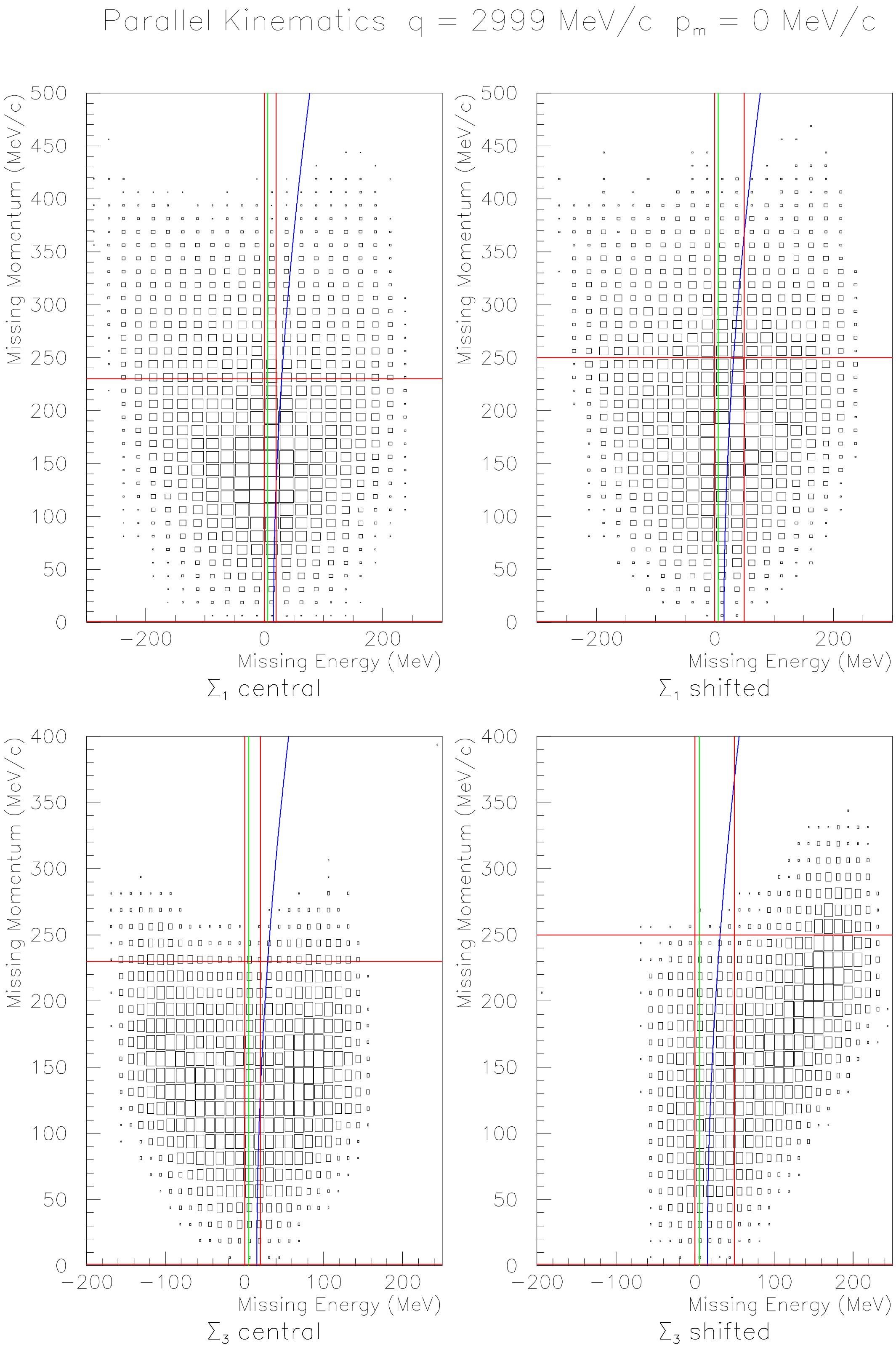
Parallel Kinematics q = 2999 MeV/c p_m = 0 MeV/c
Missing Momentum (MeV/c)
Missing Energy (MeV)
Σ1 central
Σ1 shifted
Σ3 central
Σ3 shifted

Figure 9.

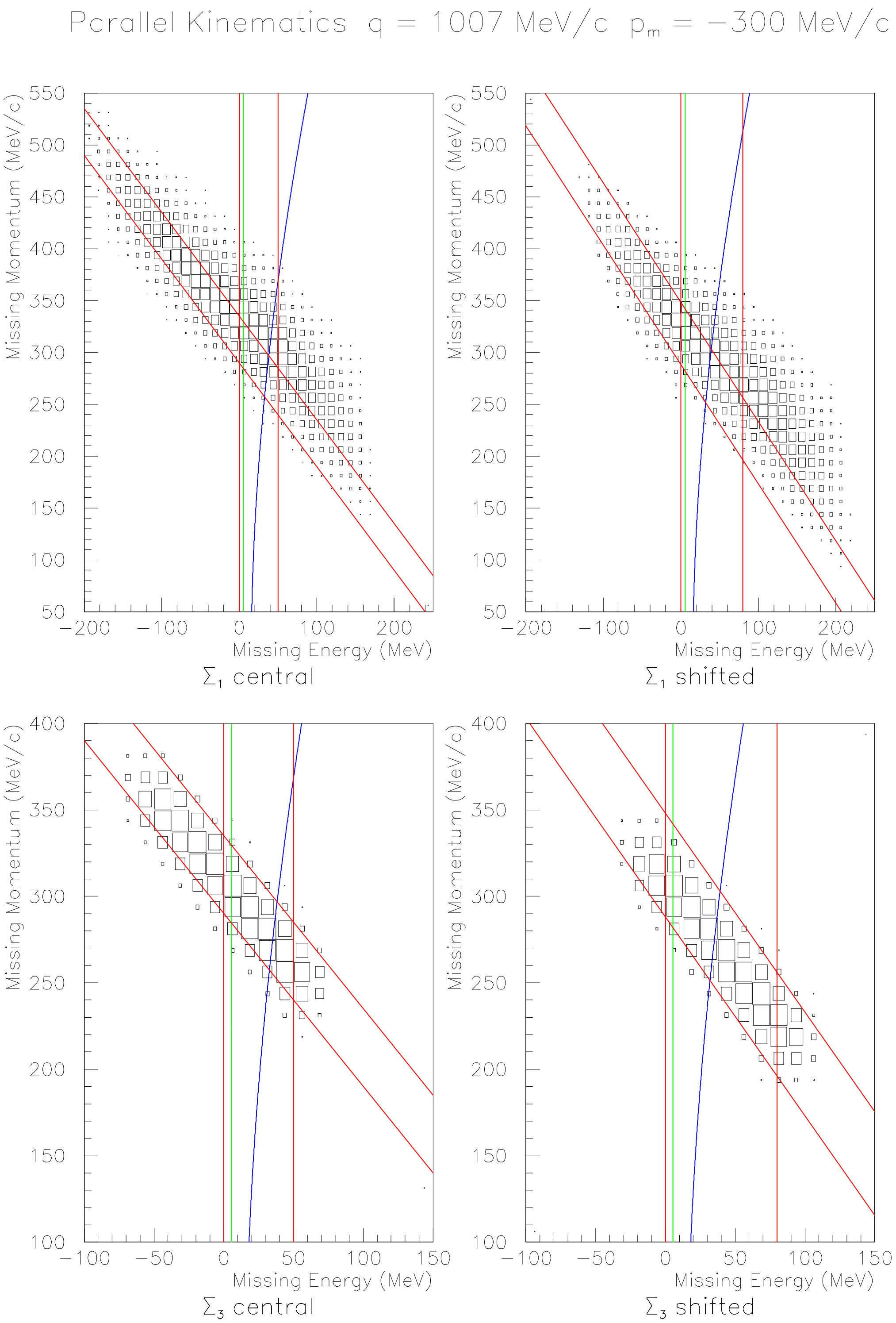

Parallel Kinematics q = 1007 MeV/c p_m = −300 MeV/c
Missing Momentum (MeV/c)
Missing Energy (MeV)
Σ₁ central
Σ₁ shifted
Σ₃ central
Σ₃ shifted

Figure 10.

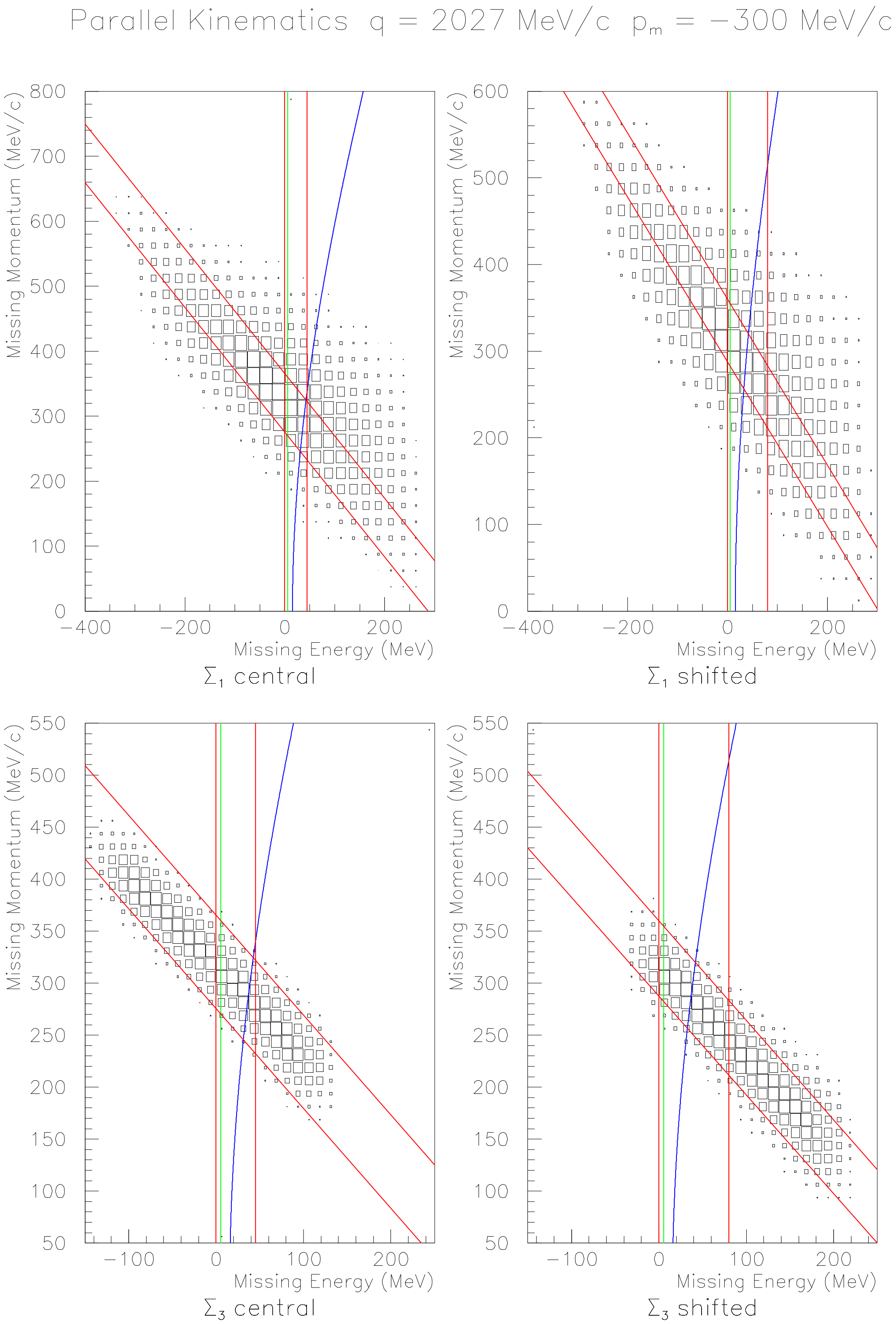
Parallel Kinematics q = 2027 MeV/c p_m = −300 MeV/c
Missing Momentum (MeV/c)
Missing Energy (MeV)
Σ_1 central
Σ_1 shifted
Σ_3 central
Σ_3 shifted
800
700
600
500
400
300
200
100
0
550
450
350
250
150
50
−400
−200
−100

Figure 11.

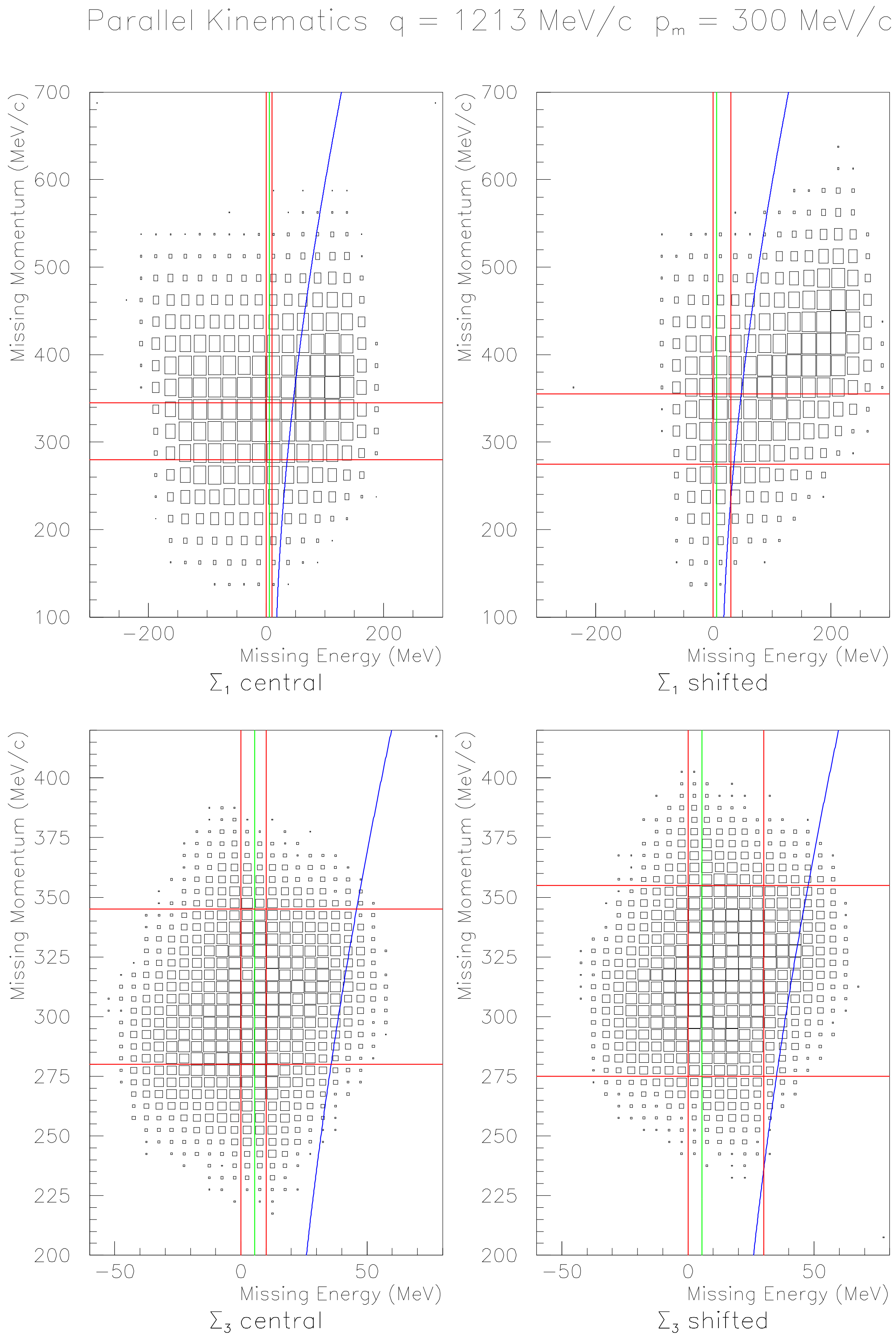
Parallel Kinematics q = 1213 MeV/c p$_m$ = 300 MeV/c
Missing Momentum (MeV/c)
Missing Energy (MeV)
Σ$_1$ central
Σ$_1$ shifted
Σ$_3$ central
Σ$_3$ shifted

Figure 12.